

Correlating Structural Order with Structural Rearrangement in Dusty Plasma Liquids: Can Structural Rearrangement be Predicted by Static Structural Information?

Yen-Shuo Su, Yu-Hsuan Liu, and Lin I

Department of Physics and Center for Complex Systems, National Central University, Zhongli, Taiwan 32001, Republic of China

(Received 2 April 2012; published 7 November 2012)

Whether the static microstructural order information is strongly correlated with the subsequent structural rearrangement (SR) and their predicting power for SR are investigated experimentally in the quenched dusty plasma liquid with microheterogeneities. The poor local structural order is found to be a good alarm to identify the soft spot and predict the short term SR. For the site with good structural order, the persistent time for sustaining the structural memory until SR has a large mean value but a broad distribution. The deviation of the local structural order from that averaged over nearest neighbors serves as a good second alarm to further sort out the short time SR sites. It has the similar sorting power to that using the temporal fluctuation of the local structural order over a small time interval.

DOI: [10.1103/PhysRevLett.109.195002](https://doi.org/10.1103/PhysRevLett.109.195002)

PACS numbers: 52.27.Lw, 61.20.-p, 64.70.pm, 82.70.Dd

Structural rearrangement (SR) at the discrete level is a ubiquitous phenomenon occurring in many strongly coupled complex systems under stochastic or slow drives. Granular systems [1,2], cold or supercooled liquids [3–7], glasses [8–12], and superconducting vortex line bundles [13], are the few good examples. Those systems share the common feature of a packed heterogeneous microstructure, composed of domains with different structural orders and different sizes. The topological constraints from the neighboring elements set up caging wells in which the element exhibits small amplitude motion (cage rattling) under perturbation. After accumulating sufficient perturbation over a certain time, the element hops over the caging barrier cooperatively with a small number of other elements [4–12,14,15]. Temporally, cage rattling and hopping (cage jumping) alternately occur. It induces stick-slip type SR through the substantial relative motion of neighboring elements.

The uncertain perturbations from the stochastic or slow drive and the complicated many-body interaction through the heterogeneous structure make predicting the uncertain SR of a local site and identifying the useful prediction alarms challenging issues. The above issues are also related to the issue of unraveling the causal correlation of some structural or dynamical variables with the subsequent substantial particle displacement [5,16,17]. For example, numerical and experimental studies on the colloidal glass of binary mixtures demonstrated that the intensities of the low frequency vibrations of particle motion are correlated with subsequent hopping and SR [10–12]. Studies on the 2D glass-forming liquids of binary mixtures revealed that the short time average of the intensities of the fast cage rattling modes is strongly correlated with later hopping, but argued against the correlation between local structure order and later dynamics [5,16,17]. On the other hand, in the recent numerical study on the 2D polydisperse glass forming liquid, the temporal average (over the structural

relaxation time scale) of the local bond-orientational order (BOO) was found to be strongly correlated with hopping [4]. The recent experimental study on the bead pile demonstrated that the slow temporal variation of the spatially averaged local structural information can be used to predict a large scale avalanche [1].

The above studies mainly correlated the temporal information of particle motion or that of structural order over a short time interval with the subsequent substantial single particle motion or SR of a local site. Whether and what kinds of the static structural information from a single snapshot of the particle image are strongly correlated with the subsequent SR, and their predicting power for local SR still remain elusive. Answering these issues also helps to understand the causal connection between static microstructure and structure dynamics.

The dusty plasma liquid (DPL) is formed by suspending micrometer sized dust particles in the low pressure discharge, through the screened Coulomb interaction between the negatively charged dusts ($\sim 10^4$ electron/dust) [18,19]. It is a good platform to study the generic behaviors of the microstructure and motion of the Yukawa liquid through direct visualization. In the past decade, the structural and dynamical heterogeneities with stick-slip avalanche cooperative hopping and SR in the cold dusty plasma liquid under different thermal excitations and external stresses have been observed and studied [6,7,18–23]. Nevertheless, the issue of predicting SR or hopping of local sites has never been explored.

In this Letter, using a cold DPL experimentally, for the first time, the causal correlation between the static local BOO and the subsequent SR of the local site is unraveled statistically by measuring histograms of the persistent time τ_p of the sustaining local BOO until the subsequent SR with a large change of BOO. Predicting short term SR using double alarms from the information of the static local BOO and its deviation from the spatially coarse grained

BOO is demonstrated, and their prediction powers are quantitatively measured. The useful coarse graining range is also identified. The results are also compared with those using the temporal fluctuation of the local BOO.

The experiment is conducted in a cylindrical symmetric rf dusty plasma system [15,24]. The weakly ionized glow discharge ($n_e \sim 10^9 \text{ cm}^{-3}$) is generated in 250 mTorr Ar gas using a 14-MHz rf power system operated at 1.6 W. Polystyrene particles ($7 \pm 0.4 \mu\text{m}$ in diameter, with a 10% standard deviation of particle diameter) are used to form the DPL. The downward ion wind toward the bottom electrode lines up dust particles into short vertical chains [15]. Dust particles along the same chain move together horizontally without vertical flipping. It makes the system a quasi-2D system [24]. The dust (chain) positions in the horizontal plane, illuminated by an expanded thin horizontal laser sheet, are digitally recorded. More details can be found in Supplemental Material [24].

The bond-orientational order $\Psi_6(\mathbf{r}_j)$ is used for measuring the local BOO: $\Psi_6(\mathbf{r}_j) = \frac{1}{N_j} \sum_k \exp(i6\theta_{jk})$, where θ_{jk} is the angle of the bond from the dust j at \mathbf{r}_j to its nearest neighbor k , and N_j is the number of its nearest neighbors [25]. $|\Psi_6| = 1$ and <0.4 for the perfect lattice site and the defect site with the nearest neighbor number deviating from six, respectively.

Figure 1(a) shows the typical snapshot of the triangulated microstructure. The color represents $|\Psi_6|$. Squares and triangles correspond to sevenfold and fivefold defects, respectively. Ordered domains with different lattice orientations and sizes coexist with defect clusters. Figures 1(b) and 1(c) show $\Delta|\Psi_6|$, the change of $|\Psi_6|$ and the dust trajectories in the subsequent 2 s. The coexisting cage rattling and cooperative hopping clusters in Fig. 1(c) manifest the dynamical heterogeneity. SRs are induced by the substantial relative displacement of adjacent particles, mainly occur in or nearby the regions with small

$|\Psi_6|$ (≤ 0.6), but also occasionally occur in the regions with large $|\Psi_6|$ [e.g., in the circled regions of Figs. 1(a)–1(c)].

The typical temporal evolution of $|\Psi_6|$ from a single dust site is shown in Fig. 1(d). The irregular bursts manifest the intermittent nature of SR. In order to unravel the causal relation between local BOO and SR, the histogram $P_{\Psi_6}(\tau_p)$ of the persistent (survival) time τ_p for a site with certain $|\Psi_6|$ at time t is measured [Fig. 2(a)]. With increasing τ , once the accumulated $\Delta|\Psi_6(\tau)| = |\Psi_6(t + \tau)| - |\Psi_6(t)|$ reaches ± 0.3 [i.e., the standard deviation of $\Delta|\Psi_6|$ at the temporal correlation time of $\Psi_6(\tau)$], it is counted as a SR event and that τ is defined as τ_p . Figure 2(a) also depicts the cumulated histograms $F_{\Psi_6}(\tau)$ of the fraction of SR events in τ , obtained by integrating $P_{\Psi_6}(\tau_p)$ from 0 to τ , at different $|\Psi_6|$. Note that, $1 - F_{\Psi_6}(\tau)$ corresponds to the survival fraction without SR after time τ . For the small $|\Psi_6|$ (< 0.6), $P_{\Psi_6}(\tau_p)$ is peaked at small τ_p (≤ 0.9 s) and has a small width. Figure 2(b) further depicts how $\langle \tau_p \rangle$ and ζ_{τ_p} , the mean and the standard deviation of τ_p , respectively, vary with $|\Psi_6|$.

The local strain energy monotonically decreases with increasing $|\Psi_6|$. Intuitively, dust particles in the region with low (high) BOO are weakly (strongly) interlocked and are more (less) likely to exhibit SR in a short time interval. This is supported by the increasing $\langle \tau_p \rangle$ with $|\Psi_6|$ in Fig. 2(b). For the site with small $|\Psi_6|$ (< 0.6), small $\langle \tau_p \rangle$ (< 1.4 s), small ζ_{τ_p} and large $F_{\Psi_6}(\tau = 2\text{s})$ (~ 0.8) indicate that small $|\Psi_6|$ can be used as a good alarm for predicting the short term (2 s) SR up to 80% certainty. For the sites with large $|\Psi_6|$, $\langle \tau_p \rangle$ and ζ_{τ_p} both increase with $|\Psi_6|$. For example, for $|\Psi_6| = 0.7$, 50% of SR occurs within $\tau = 2$ s. For $|\Psi_6| = 0.9$, $P_{\Psi_6}(\tau_p)$ has a quite flat distribution for $\tau_p > 1$ s. Although $F_{\Psi_6}(\tau = 2\text{s})$ (~ 0.25) at $|\Psi_6| = 0.9$ indicates only a small portion of SR occurring in 2 s, the large $\langle \tau_p \rangle$ with large ζ_{τ_p} implies that $|\Psi_6|$ is not a good

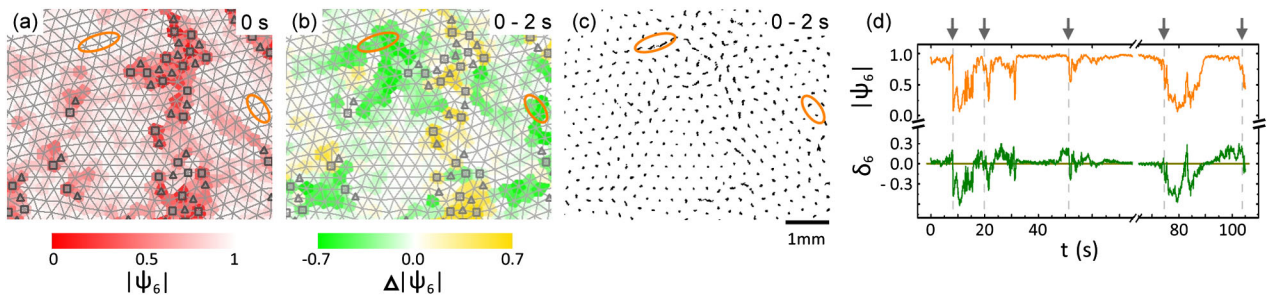


FIG. 1 (color online). (a) The triangulated snapshot of the microstructure at $t = 0$ s, with squares and triangles representing the sevenfold and the fivefold defects, respectively, and the color representing the local $|\Psi_6|$. (b) The contour plot showing the change of $|\Psi_6|$, $\Delta|\Psi_6|$ from 0 to 2 s. The background triangulated grids depict the initial microstructure. SR mainly occurs in the form of clusters, in or nearby the regions with small $|\Psi_6|$ (≤ 0.6), and occasionally inside the ordered regions (e.g., the circled regions) with large $|\Psi_6|$. (c) Dust trajectories from 0 to 2 s. (d) The typical temporal evolutions of $|\Psi_6|$ and δ_6 of a particle, where δ_6 is the deviation of the $|\Psi_6|$ of the tested site from the coarse grained $|\Psi_6|$, over the sites inside the circle 1.3 a in radius. Most SR events are led by small $|\Psi_6|$ (< 0.6). The arrows show the examples of the SR events led by the large $|\Psi_6|$, where the additional information of δ_6 are needed as the additional alarm.

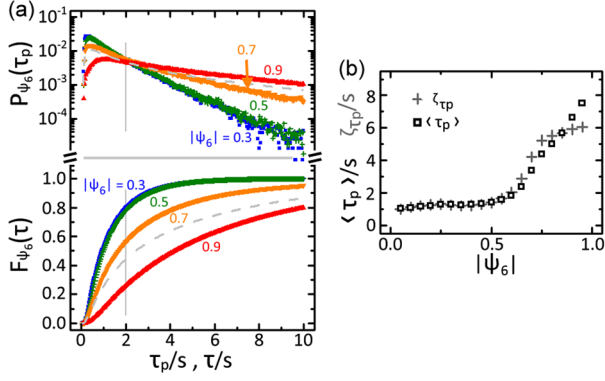


FIG. 2 (color online). (a) The histograms $P_{\Psi_6}(\tau_p)$ and the cumulated histograms $F_{\Psi_6}(\tau)$ at different $|\Psi_6|$, respectively. $F_{\Psi_6}(\tau)$ is the fraction of SR events occurring in time interval τ . The gray dashed curves are the corresponding histograms for all the sites without using $|\Psi_6|$ for sorting. (b) $\langle \tau_p \rangle$ and ζ_{τ_p} , the mean and the standard deviation of τ_p respectively, versus $|\Psi_6|$. The small $|\Psi_6|$ (< 0.6) is a good alarm to predict the short term SR up to 80% certainty. For the site with large $|\Psi_6| > 0.6$, the large $\langle \tau_p \rangle$ with the large ζ_{τ_p} reflects the large uncertainty of predicting SR.

alarm to predict τ_p for SR with high certainty. Namely, unlike the intuitive expectation, high BOO does not guarantee the high stability of the local site.

For the sites with high BOO, can we further find a second alarm to sort out those having a larger tendency for the short term SR, from the wide spread distribution of τ_p ? For a coupled system, the local dynamical evolution is mainly determined by the forces from particles in the surrounding network over an extended scale, in addition to the stochastic or other slow drives. The insufficient information from the local $|\Psi_6|$, which decreases with the increasing local strain, only provides limited prediction power. The structural or dynamical information over certain spatial or temporal scales are needed. Israeli *et al.* numerically demonstrated that the irreducible physical processes in a complex system is predictable at a coarse grained level [26].

Based on this idea, we test the effect of the second alarm δ_6 , the deviation of the $|\Psi_6|$ of the tested site from the coarse grained $|\Psi_6|$, over the sites inside the circle $1.3a$ in radius (i.e., further including BOOs of the nearest neighbors). Figure 1(d) shows the temporal evolution of δ_6 . The events with sudden drops of large $|\Psi_6|$ as indicated by the arrows are usually led by the rises of δ_6 . It evidences that δ_6 helps to more clearly sort out short term SR events from the sites with large $|\Psi_6|$. Figure 3(a) depicts the conditional histograms of τ_p , $p_{\delta_6}(\tau_p)$, and the conditional cumulated histograms $f_{\delta_6}(\tau)$ of the fraction of SR events under different δ_6 , for $|\Psi_6| = 0.9$. The width of $p_{\delta_6}(\tau_p)$ decreases with increasing δ_6 . Figure 3(b) indicates that, for $|\Psi_6| = 0.9$, $\langle \tau_p \rangle$ and $f_{\delta_6}(\tau = 2s)$ drastically decrease and

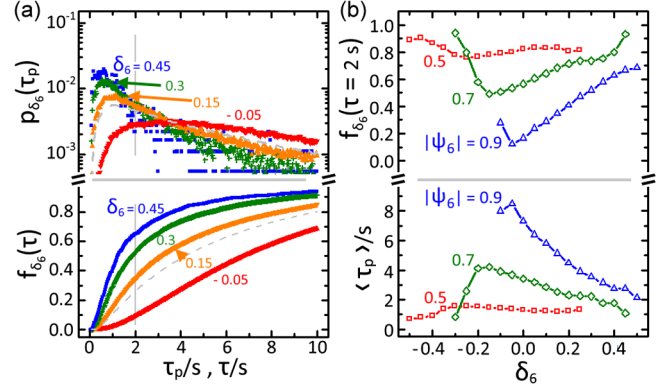


FIG. 3 (color online). (a) The conditional histograms of τ_p , $p_{\delta_6}(\tau_p)$, and the conditional cumulated histograms $f_{\delta_6}(\tau)$ of the fraction of SR events in τ , under different δ_6 , for $|\Psi_6| = 0.9$. The gray dashed curves correspond to $P_{\Psi_6}(\tau_p)$ and $F_{\Psi_6}(\tau)$ of all the sites with $|\Psi_6| = 0.9$, without using the second alarm δ_6 . (b) $f_{\delta_6}(\tau = 2s)$ and $\langle \tau_p \rangle$ versus δ_6 at different $|\Psi_6|$. The solid lines are used for eye guiding. The large δ_6 serves as a good second alarm to sort out the short term SR sites with $|\Psi_6| > 0.6$.

increase by factors of four and six, respectively, as δ_6 increases from 0 to 0.5. In 2 s, 70% SR occurs for $\delta_6 = 0.45$, but 12% SR occurs for $\delta_6 = -0.05$.

How do we explain the above observations? δ_6 provides the information of the deviation of the local BOO from the mean BOO of the nearest neighbors. It helps to distinguish whether a site with high BOO is sitting away or near the disorder sites which have short τ_p . For the site with large $|\Psi_6|$, the large δ_6 indicates that the site is surrounded by large numbers of neighbors with poor BOO. SR easily occurs through the propagation of high rate SR from adjacent disordered sites [27]. It drastically reduces $\langle \tau_p \rangle$. Namely, SR also occurs cooperatively in the form of small avalanched like clusters [7]. An ordered site could also exhibit short term SR due to the small τ_p of the neighboring disordered site. The increasing $\langle \tau_p \rangle$ with decreasing δ_6 implies that the background sites with more homogeneous structural order can sustain longer structural memory. For $|\Psi_6| = 0.7$, the drop of $\langle \tau_p \rangle$ with decreasing δ_6 beyond -0.2 can be attributed to the increasing rate of SR which increases $|\Psi_6|$ to those of surrounding sites with better BOO. For the disordered site with small $|\Psi_6|$ (< 0.6), the poor interlocking makes it hard to keep the structural memory. The weak effect of the mean BOO of the nearest neighbors leads to the small change of $\langle \tau_p \rangle$ and $f_{\delta_6}(\tau = 2s)$ in Fig. 3(b). This also agrees with the small $\langle \tau_p \rangle$ and ζ_{τ_p} found in Fig. 2(b). Note that we also found that increasing the coarse graining radius deteriorates the predicting power of the short term SR at large δ_6 and the resolving power of $\langle \tau_p \rangle$ (see Fig. S2 of Supplemental Material [24]). Namely, the BOOs of the nearest neighbor sites play the key role determining the short term SR of the local site with good BOO.

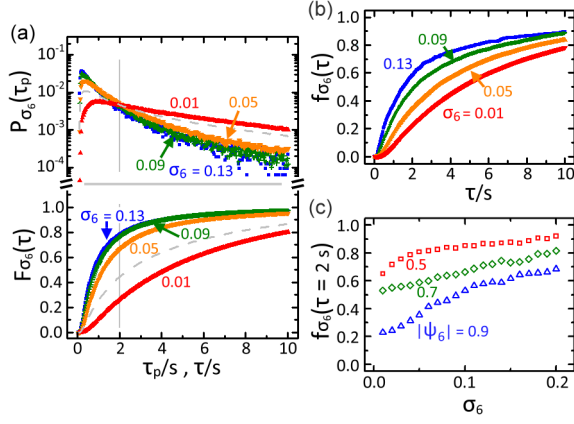


FIG. 4 (color online). (a) The histograms $P_{\sigma_6}(\tau_p)$ and the cumulated histograms $F_{\sigma_6}(\tau)$ at different fixed σ_6 , respectively, using σ_6 as a single indicator for predicting SR. $F_{\sigma_6}(\tau)$ is the fraction of SR events integrated over τ . The gray dashed curves correspond to $P(\tau_p)$ and $F(\tau)$, for all the sites without using any indicator. (b) The conditional cumulated histograms $f_{\sigma_6}(\tau)$ at $|\Psi_6| = 0.9$ and different σ_6 . (c) $f_{\sigma_6}(\tau = 2s)$ versus σ_6 at different $|\Psi_6|$. Similarly to δ_6 , σ_6 has strong influence on sorting out the short term SR sites from the sites with large $|\Psi_6|$.

The recent study on propensity for the glass forming binary liquid showed that the intensity of the fast rattling mode of single particle motion within a small time interval is strongly correlated with subsequent single particle hopping [5,16,17]. Since SR is from the relative motion of adjacent particles, the above finding makes it interesting to check the prediction power for short term SR using the temporal information of $|\Psi_6|$ and how it compares with those using static BOO in our above studies. The standard deviation of the fluctuation of $|\Psi_6|$, σ_6 , in 0.3 s interval before t is chosen for the test. Figure 4(a) shows that, similarly to using $|\Psi_6|$ as a single alarm, σ_6 alone is a good alarm for the short time SR only when it is large (80% of SR occur in 2 s for $\sigma_6 > 0.09$), but not small (see the wide spread τ_p for $\sigma_6 = 0.01$). However, Figs. 4(b) and 4(c) show that, as the second alarm associated with the first alarm $|\Psi_6|$, σ_6 also provides the similar power of sorting out the short term SR (small τ_p) sites which have large $|\Psi_6|$, compared to that using δ_6 . For example, for $|\Psi_6| = 0.9$, $f_{\sigma_6}(\tau = 2s)$ increases from 0.2 to 0.7 as σ_6 increases from 0.01 to 0.2 [Fig. 4(c)], and $f_{\delta_6}(\tau = 2s)$ increases from 0.12 to 0.7 as δ_6 increases from -0.05 to 0.45 [Fig. 3(b)]. Namely, the above finding implies that the sites with large $|\Psi_6|$ and large δ_6 are more floppy and have higher tendency to exhibit the larger level of fast temporal fluctuation of BOO, right before the following short term SR.

In conclusion, whether and what kinds of the static structural information from a single snapshot of particle image are strongly correlated with the subsequent SR and their predicting power for SR are investigated experimentally in the quenched dusty plasma liquid. The major

findings are listed as follows: (a) The low local BOO is a good alarm for predicting the short term SR. (b) For the sites with high BOO ($|\Psi_6| > 0.6$), $\langle \tau_p \rangle$ is large. However, unlike the intuitive expectation, a large fraction of sites still exhibit short term SR. The deviation from the BOO averaged over the nearest neighbors serves as a good second alarm for further sorting out the short term SR sites. (c) The predicting power of the above second alarm is similar to that using the temporal fluctuation of local BOO. It manifests that the spatially and the temporally coarse grained information of BOO are both useful for sorting out the floppy spots exhibiting short term SR, from the sites with high BOO.

This work is supported by the National Science Council of the Republic of China, under Contract No. NSC-99-2112-M-008-002-MY3.

- [1] O. Ramos, E. Altshuler, and K. J. Maloy, *Phys. Rev. Lett.* **102**, 078701 (2009).
- [2] R. Candelier, O. Dauchot, and G. Biroli, *Phys. Rev. Lett.* **102**, 088001 (2009).
- [3] C. Reichhardt and C. J. Olson Reichhardt, *Phys. Rev. Lett.* **90**, 095504 (2003).
- [4] T. Kawasaki, T. Araki, and H. Tanaka, *Phys. Rev. Lett.* **99**, 215701 (2007).
- [5] R. Candelier, A. Widmer-Cooper, J. K. Kummerfeld, O. Dauchot, G. Biroli, P. Harrowell, and D. R. Reichman, *Phys. Rev. Lett.* **105**, 135702 (2010).
- [6] W. Y. Woon and L. I., *Phys. Rev. Lett.* **92**, 065003 (2004); C. L. Chan and L. I., *Phys. Rev. Lett.* **98**, 105002 (2007).
- [7] C. L. Chan, W. Y. Woon and L. I., *Phys. Rev. Lett.* **93**, 220602 (2004).
- [8] R. Besseling, E. R. Weeks, A. B. Schofield, and W. C. K. Poon, *Phys. Rev. Lett.* **99**, 028301 (2007).
- [9] P. Schall, D. A. Weitz, and F. Spaepen, *Science* **318**, 1895 (2007).
- [10] M. L. Manning and A. J. Liu, *Phys. Rev. Lett.* **107**, 108302 (2011).
- [11] K. Chen, M. L. Manning, P. J. Yunker, W. G. Ellenbroek, Z. Zhang, A. J. Liu, and A. Yodh, *Phys. Rev. Lett.* **107**, 108301 (2011).
- [12] A. Ghosh, V. Chikkadi, P. Schall, and D. Bonn, *Phys. Rev. Lett.* **107**, 188303 (2011).
- [13] I. Guillamon, H. Suderow, S. Vieira, J. Sesé, R. Córdoba, J. M. De Teresa, and M. R. Ibarra, *Phys. Rev. Lett.* **106**, 077001 (2011).
- [14] E. R. Weeks, J. C. Crocker, A. C. Levitt, A. Schofield, D. A. Weitz, *Science* **287**, 627 (2000).
- [15] Y. J. Lai and L. I., *Phys. Rev. Lett.* **89**, 155002 (2002); Y. J. Lai and L. I., *Phys. Rev. Lett.* **89**, 155002 (2002); Y. S. Su, C. W. Io, and L. I., *Phys. Rev. E* **86**, 016405 (2012).
- [16] A. Widmer-Cooper and P. Harrowell, *Phys. Rev. Lett.* **96**, 185701 (2006).
- [17] L. Berthier and R. L. Jack, *Phys. Rev. E* **76**, 041509 (2007).

- [18] G.E. Morfill and A.V. Ivlev, *Rev. Mod. Phys.* **81**, 1353 (2009), and the references there in.
- [19] C.L. Chan, C.W. Io, and L.I., *Contrib. Plasma Phys.* **49**, 215 (2009), and the references there in.
- [20] Z. Donko, J. Goree, P. Hartmann, and K. Kutasi, *Phys. Rev. Lett.* **96**, 145003 (2006).
- [21] S. Ratynskaia, K. Rypdal, C. Knapek, S. Khrapak, A.V. Milovanov, A. Ivlev, J.J. Rasmussen, and G.E. Morfill, *Phys. Rev. Lett.* **96**, 105010 (2006).
- [22] Z. Donko and P. Hartmann, *Phys. Rev. E* **78**, 026408 (2008).
- [23] K. Rypdal, B. Kozelov, S. Ratynskaia, B. Klumov, C. Knapek, and M. Rypdal, *New J. Phys.* **10**, 093018 (2008).
- [24] See Supplemental Material at <http://link.aps.org/supplemental/10.1103/PhysRevLett.109.195002> for the details of experimental setup, results, and discussion.
- [25] K.J. Strandburg, *Bond-Orientational Order in Condensed Matter Systems* (Springer, New York, 1992).
- [26] N. Israeli and N. Goldenfeld, *Phys. Rev. Lett.* **92**, 074105 (2004).
- [27] C.H. Chiang and L.I., *Phys. Rev. Lett.* **77**, 647 (1996).